# Protein−DNA Chimeras for Nano Assembly

Diana A. Pippig,[†,*] Fabian Baumann,[†] Mathias Strackharn,[†,§] Daniela Aschenbrenner,[†,‡] and Hermann E. Gaub[†,*]

[†]Center for Nanoscience and Department of Physics, University of Munich, Amalienstraße 54, 80799 Munich, Germany and [‡]Center for Integrated Protein Science, 81377 Munich, Germany. [§]Present address: Scanlab AG, Siemensstr. 2a, 82178 Puchheim, Germany.

ABSTRACT In synthetic biology, "understanding by building" requires exquisite control of the molecular constituents and their spatial organization. Site-specific coupling of DNA to proteins allows arrangement of different protein functionalities with emergent properties by self-assembly on origami-like DNA scaffolds or by direct assembly *via* Single-Molecule Cut & Paste (SMC&P). Here, we employed the ybbR-tag/Sfp system to covalently attach Coenzyme A-modified DNA to GFP and, as a proof of principle, arranged the chimera in different patterns by SMC&P. Fluorescence recordings of individual molecules proved that the proteins remained folded and fully functional throughout the assembly process. The high coupling efficiency and specificity as well as the negligible size (11 amino acids) of the ybbR-tag represent a mild, yet versatile, general and robust way of adding a freely programmable and highly selective attachment site to virtually any protein of interest.
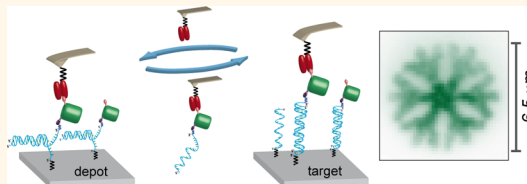
KEYWORDS: protein−DNA chimera · single-molecule cut & paste · AFM · spatial arrangement · patterning · single-molecule fluorescence

To study protein networks at the single molecule level, precise targeting and localization of its constituents are indispensable prerequisites. To this end, we developed the Single-Molecule Cut & Paste (SMC&P) technique,[1,2] which combines the angstrom level precision of the scanning probe microscope with the selectivity of bio−molecular interactions for the assembly of molecules in arbitrary arrangements. It allows individual molecules to be picked up from a depot area and assembled one by one at a chosen position in a "construction site" in the target area (Scheme 1).

SMC&P is based on noncovalent, but thermally stable, bonds for storage (depot), handling (AFM cantilever), and deposition (target). These bonds are chosen such that the force required to release the storage interaction is lower than the force required to overcome the handle attachment, which again is lower than the deposition bond ($F_s < F_h < F_d$). For one-by-one assembly, the functionalized AFM cantilever tip is allowed to bind a transfer molecule in the depot area *via* the specific handle. Upon retraction the storage bond ruptures, the transfer molecule remains attached to the cantilever and is then transferred to the construction site.

There, the AFM tip is lowered and the transfer molecule forms a deposition bond and is thus placed at a chosen position in the construction site. Upon retraction of the tip, the handle bond ruptures, while the transfer molecule remains at its position, and the AFM tip is free again to pick up a new transfer molecule from the depot area. Remarkably, the system is now in the same state as prior to the first pick-up so that the SMC&P-process may be repeated with the same tip in a cyclic manner. The rupture forces in this hierarchical system, which allow this cut and paste process to be run over thousands of cycles, may either be programmed by the selection of the binding partners or predetermined by the force loading rates.[3−6] Note that for each of these bond-rupture processes a force *versus* distance curve is recorded to verify that indeed individual molecules were handled or, in the case of high density tip functionalization, to provide an estimate of the number of transferred molecules per cycle.
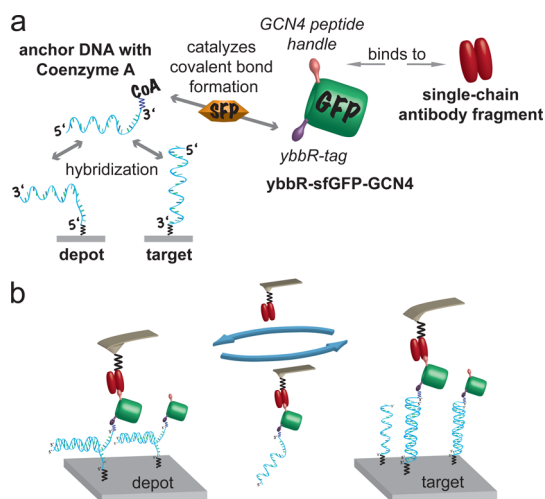
During recent years, this method was improved and taken from the initial DNA-based stage *via* the functional assembly of RNA aptamers[7] to the much more complex protein level.[8,9] The first approach in protein

Scheme 1. SMC&P with a chimeric GFP−DNA moiety. (a) To ensure a hierarchical force distribution, DNA duplex interaction is utilized in depot and target region, with the DNA in zipper ($F_{rupture} \sim 20$ pN)[3] and shear conformation ($F_{rupture} \sim 65$ pN),[4] respectively. The intermediate force for the transport handle was achieved using an anti-GCN4-peptide single-chain antibody fragment ($F_{rupture} \sim 50$ pN).[5] (b) Principle of repeatable transfer cycling in protein SMC&P experiments.

SMC&P relied on the use of Zincfinger fusion proteins.[9] The Zincfinger moiety and its specifically bound DNA transfer strand acted as a shuttle for other proteins of interest, combining the advantages and reproducibility of DNA-only SMC&P with the ability to selectively collect and deposit single proteins without loss of functionality. The need for an even more versatile protein transport system arises from the size of the Zincfinger, which imposes a rather big alteration to the protein of interest; its poor solubility, especially in combination with more complex protein candidates; and the noncovalent nature of its DNA interaction.

Minimal modification of the proteins of interest, as well as covalent attachment to the DNA carrier, is greatly desirable. Moreover, there is a general need for robust strategies to selectively couple DNA to proteins. Such chimeras are extremely useful in immunobiological applications[10,11] as well as nanobiotechnology,[12] e.g., for the DNA origami technology.[13] Since the various options to couple DNA-oligocleotides to proteins harbor certain drawbacks, no gold standard exists hitherto.

Click-chemistry,[14] e.g., while being very specific and selective itself, requires less selective modification of amino acid side chains[15] or the incorporation of non-natural amino acids into proteins.[16,17] The latter is often laborious in terms of expression system and yield.[18] Furthermore, reaction conditions can be rather harsh for proteins or relatively inefficient.[19] Coupling strategies involving bifunctional cross-linkers are less specific. Attachment can be achieved via either primary amino groups in proteins or thiol groups, which often requires incorporation of a single accessible cysteine and mutation of others. Thus, full integrity and functionality of the modified proteins is not guaranteed or even unlikely. Furthermore, suicide enzymes, e.g., HaloTag or SNAP-tag (hAGT), could be employed as fusion protein tags for site-specific immobilization reactions.[20−22] However, their respective sizes of 33 and 20 kDa diminish their attractiveness for single-protein manipulation.

We thus chose to employ the 11 amino acid ybbR-tag that, assisted by the Phosphopantetheinyl Transferase Sfp,[23] allows for the site-selective attachment of Coenzyme A (CoA)-modified DNA to proteins of interest[24] (Scheme 1). Coenzyme A is easily reacted to commercially available Maleimide-modified oligonucleotides via its intrinsic thiol group, and the already-coupled construct is available upon request for purchase from several companies. The ybbR-tag technology is widely used for labeling proteins with, e.g., biotin or fluorescent dyes and works efficiently on either N- or C-terminus or accessible unstructured regions of proteins.[25] The ybbR-tag/Sfp system can be further employed in the immobilization of proteins on Coenzyme A-functionalized solid carriers or surfaces.[26−28]

RESULTS AND DISCUSSION

We expressed GFP with an N-terminal ybbR-tag and a C-terminal short GCN4-tag and reacted the construct with Coenzyme A-modified transfer-DNA with high yield (Supporting Information Figure S1). The purified chimera was then successfully incorporated in SMC&P experiments. Transport processes were extremely efficient, and the GFP remained intact and fluorescent throughout the SMC&P procedure (Figures 1a,b, and 2). The number of transported molecules can be easily tuned by using either different cantilever sizes and/or varying functionalization densities at the cantilever tip (Figures 1 and 2). Glass surface functionalization is kept as dense as possible to allow for a homogeneous distribution of transfer-DNA:protein complex binding sites in the depot and target area. The number of deposited protein molecules is thus solely dependent on the number of GCN4-binding antibody anchors on the cantilever tip.

To achieve the highest precision possible and to prove that individual molecules can be transported, we performed SMC&P of the GFP-DNA chimera employing BioLever Mini (BLM) cantilevers. Such cantilevers harbor extremely sharp and small, but still functionalizable, tips (10 nm nominal tip radius of curvature; sharpened from the initial pyramidal shape by an oxidation process) and hence, offer the highest accuracy in molecule deposition. Grid patterns of 8×8 distinct transfer sites (10.5×10.5 μm in size, 1.5 μm in each direction between each grid point) were assembled (Figure 1 and Supporting Information Figure S2). The transport process was followed directly by recording force distance curves with the AFM during SMC&P
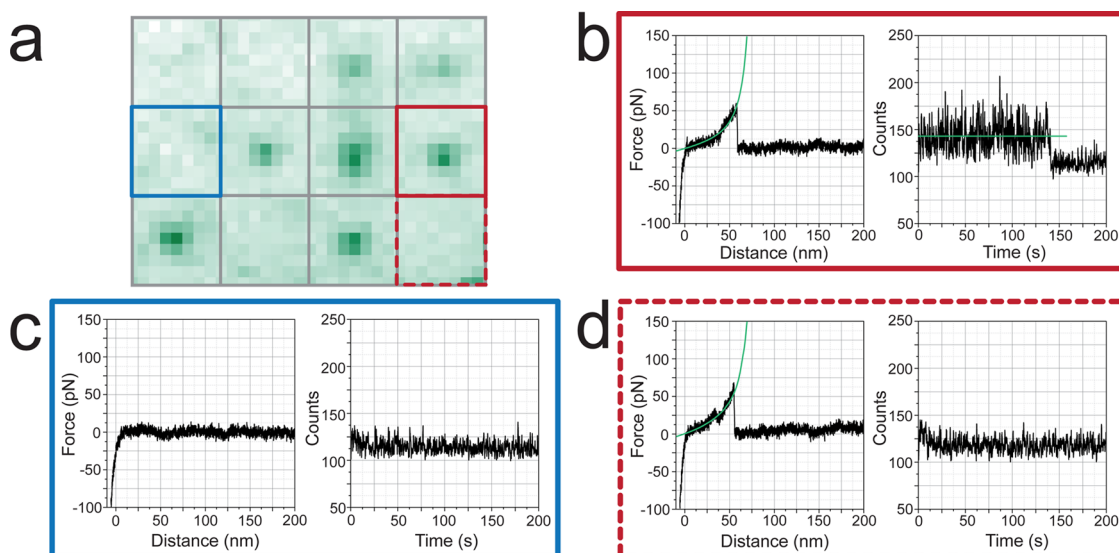
Figure 1. Individual GFP molecules can be transported with AFM cantilevers. (a) Representative 3 × 4 deposition point grid section obtained by SMC&P of GFP molecules employing a BLM cantilever (standard deviation of the fluorescence signal over 100 s, ImageJ) with 7 observable GFP signals out of 12 transfer cycles. (b) Rupture forces around 50 pN (at loading rates around 300 pN/s) correspond to single deposition events in the target area and correlate with a single bleaching step in the fluorescence signal over time at the distinct deposition point (2 × 2 pixel area). (c) Target force curves showing no force built-up correspond to cycles where no molecule could be deposited, which is also evident from the lack of a fluorescence signal at the respective grid position. (d) Due to its limited photostability, a fraction of the GFP molecules is expected to already be bleached throughout the purification and SMC&P preparation process. Yet, the dual mode of transport observation—directly following force−distance curves while performing SMC&P and subsequent fluorescence imaging—allows the detection of single GFP deposition events, even in the absence of a fluorescence signal.
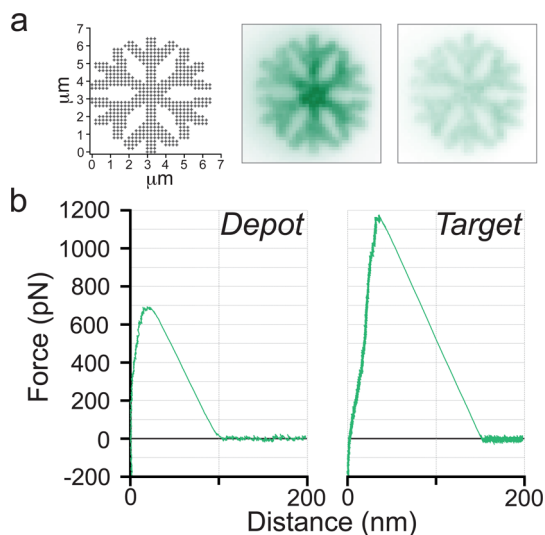
Figure 2. High transport efficiency protein SMC&P. (a) After exposure of the 552-point deposition snowflake pattern for 60 s (0.1 s exposure time at ∼10 W/cm²), it still appears homogeneous and clearly discernible. The pattern template and the average fluorescence over the first (bright) and last (faint) 20 frames of the TIRFM acquisition (600 frames at 0.1 s exposure time) are depicted. (b) Judging from extremely high rupture forces, several (>20) GFP molecules were transported in each cycle.

cycling (Figure 1 and Supporting Information Figure S3). The pattern was subsequently imaged by TIRF microscopy (Figure 1a and Supporting Information Figure S2a). The number of deposited GFP molecules arises from the fluorescence signal over time at a

distinct grid point (Figure 1b). We could thus show that indeed single molecules were transferred. Notably, SMC&P utilizing such sharp-tipped cantilevers can also result in force curves devoid of any rupture event and thus no GFP deposition (Figure 1c). In some cases, even though single rupture events were observed, no fluorescence signal could be detected at the corresponding grid position (Figure 1d). A likely cause is the limited photostability of GFP. A fraction of the GFP molecules can be expected to already undergo photobleaching during the purification and SMC&P preparation process. Thus, nonfluorescent GFP molecules would be occasionally transported as well. Furthermore, the rupture events underlying the SMC&P procedure only have a certain probability to lie in the expected force range. In rare cases, the observed rupture event for the deposition process could therefore theoretically originate from a rupture of the shear DNA deposition bond (a most probable rupture force ∼65 pN would be expected for the utilized 40 bp duplex at the observed loading rates around 300 pN/s)[4] instead of the desired antibody fragment/GCN4-peptide dissociation ($F_{rupture}$ ∼ 50 pN at the observed loading rates around 300 pN/s).[5] This would result in the GFP-DNA chimera remaining on the cantilever and could hence also account for the absence of a fluorescence signal in the respective grid position.

In a typical SMC&P experiment where a 64-point distinct deposition pattern was assembled, an average of 0.89 molecules per cycle were picked up from the

depot area, judging from the according force spectroscopy data. More relevantly, an average of 0.84 molecules were deposited per cycle, based on rupture force evaluation. A fluorescence-based assessment of the number of transported and actually deposited molecules gives rise to an average value of 0.5 molecules per cycle (Supporting Information Figure S2). For comparison, in former DNA-only SMC&P experiments, employing AFM probes with broader tips, around 0.5 molecules per cycle were transported.[29] Further, in earlier Zincfinger-based protein-SMC&P approaches, where larger numbers of molecules should be transferred with densely functionalized broad-tipped cantilevers, efficiencies ranged around 2 molecules per cycle.[9]

Conditions are optimized in a way that mostly individual molecules are transported. Rarely, the transport of two molecules per cycle is observed, whereas SMC&P cycles devoid of a deposition event are much more likely to occur. A transport efficiency of less than one molecule per cycle is acceptable for the benefit of being able to frequently transport truly individual protein constructs. Under the given conditions, one SMC&P cycle takes less than 3 s. This is mainly affected by the chosen pulling speeds that are optimized with respect to apparent loading rates and thus probable rupture forces. These parameters require careful adjustment to ensure functional and structural integrity of the transported protein as well as balancing the hierarchical rupture force "triangle" the SMC&P principle builds-up on. Binding kinetics of the interacting molecules are not expected to be limiting under the experimental conditions (see Supporting Information, p S7).

To further demonstrate the robustness of the SMC&P setup, we additionally utilized a pyramidal shaped MLCT cantilever probe with a nominal tip curvature radius of approximately 20 nm to assemble the pattern of a snowflake in 552 transfer cycles (Figure 2). GFP fluorescence of the pattern was extremely strong, and after laser exposure at 10 W/cm^2 for 60 s, the homogeneous pattern was still clearly discernible (Figure 2). Considering GFP's limited photostability, this indicates high transport efficiency. Judging from AFM rupture force curves of this experiment, more than 20 molecules were transported per cycle.

CONCLUSIONS

In conclusion, we have largely improved protein-based SMC&P in terms of versatility, precision, efficiency and robustness. The adaptability of the system will in the future allow tackling of any protein of interest in single-molecule studies or in complex protein networks, spatially arranged by means of SMC&P. Moreover, protein SMC&P can be utilized to for example place individual enzymes in the center of bow-tie nanoantenna structures[30] or Zero-Mode Waveguides (ZMW), as has been demonstrated for DNA.[31] In favor of this, the applicability of cantilever tips with a high aspect ratio is especially crucial for protein SMC&P as the cantilevers with larger pyramidal shaped tips exceed the dimensions of the nanometer-sized holes of ZMWs. The precision and spatial control achieved with protein SMC&P will thereby significantly improve enzymatic studies in the presence of high concentrations of fluorescent substrates that are unmet by other single-molecule fluorescence methods.[32]

Importantly, the protein−DNA coupling strategy employing Coenzyme A-modified DNA and the ybbR-tag/Sfp system proved to be high-yielding, straightforward (also with other protein constructs, data not shown), and relatively inexpensive in terms of material costs and time. It thus promises to be a useful tool in providing protein−DNA chimeras, which should also be advantageous for other fields of nanobiotechnology and protein engineering.

EXPERIMENTAL SECTION

SMC&P experiments were carried out on a combined AFM/TIRFM setup, as described previously[1] and detailed information can be found in the Supporting Information. In short, GFP harboring an N-terminal Hexa-His-tag, followed by an 11 amino acid ybbR-tag[25] and a C-terminal GCN4-tag[5] was expressed in *Escherichia coli* BL21 DE3 CodonPlus and purified according to standard protocols. The construct was then reacted with Coenzyme A-modified transfer-DNA (biomers.net GmbH, Ulm, Germany) in the presence of Sfp. The progress of the coupling reaction was assessed by SDS-PAGE and subsequent fluorescence scanning as well as Coomassie staining of gels. The GFP−DNA chimera was then purified by anion exchange chromatography. The construct was bound to the DNA-depot area on a functionalized glass surface *via* a custom-built microfluidic system. SMC&P was achieved by means of anti-GCN4 antibody functionalized cantilever tips, delivering GFP−DNA molecules from the depot area to the construction site in the target area. BLM cantilevers were used to transport individual GFP−DNA chimeras. MLCT cantilevers were utilized for comparison and high transport efficiencies. Molecule pick-up and deposition was followed directly by AFM force−distance curves, and the assembled pattern was imaged by TIRF microscopy subsequent to the writing process. Simultaneous detection of AFM curves and fluorescence is also possible; however, it was not feasible for GFP due to its relatively low photostability.

REFERENCES AND NOTES

1. Kufer, S. K.; Puchner, E. M.; Gumpp, H.; Liedl, T.; Gaub, H. E. Single-Molecule Cut-and-Paste Surface Assembly. *Science* **2008**, *319*, 594–596.
2. Puchner, E. M.; Kufer, S. K.; Strackharn, M.; Stahl, S. W.; Gaub, H. E. Nanoparticle Self-Assembly on a DNA-Scaffold Written by Single-Molecule Cut-and-Paste. *Nano Lett.* **2008**, *8*, 3692–3695.
3. Rief, M.; Clausen-Schaumann, H.; Gaub, H. E. Sequence-Dependent Mechanics of Single DNA Molecules. *Nat. Struct. Biol.* **1999**, *6*, 346–349.
4. Morfill, J.; Kuhner, F.; Blank, K.; Lugmaier, R. A.; Sedlmair, J.; Gaub, H. E. B-S Transition in Short Oligonucleotides. *Biophys. J.* **2007**, *93*, 2400–2409.
5. Morfill, J.; Blank, K.; Zahnd, C.; Luginbuhl, B.; Kuhner, F.; Gottschalk, K. E.; Pluckthun, A.; Gaub, H. E. Affinity-Matured Recombinant Antibody Fragments Analyzed by Single-Molecule Force Spectroscopy. *Biophys. J.* **2007**, *93*, 3583–3590.
6. Dudko, O. K.; Hummer, G.; Szabo, A. Intrinsic Rates and Activation Free Energies from Single-Molecule Pulling Experiments. *Phys. Rev. Lett.* **2006**, *96*, 108101.
7. Strackharn, M.; Stahl, S. W.; Puchner, E. M.; Gaub, H. E. Functional Assembly of Aptamer Binding Sites by Single-Molecule Cut-and-Paste. *Nano Lett.* **2012**, *12*, 2425–2428.
8. Strackharn, M.; Stahl, S. W.; Severin, P. M.; Nicolaus, T.; Gaub, H. E. Peptide-Antibody Complex as Handle for Single-Molecule Cut & Paste. *ChemPhysChem* **2012**, *13*, 914–917.
9. Strackharn, M.; Pippig, D. A.; Meyer, P.; Stahl, S. W.; Gaub, H. E. Nanoscale Arrangement of Proteins by Single-Molecule Cut-and-Paste. *J. Am. Chem. Soc.* **2012**, *134*, 15193–15196.
10. Akter, F.; Mie, M.; Grimm, S.; Nygren, P. A.; Kobatake, E. Detection of Antigens Using a Protein-DNA Chimera Developed by Enzymatic Covalent Bonding with Phix Gene A. *Anal. Chem.* **2012**, *84*, 5040–5046.
11. Burbulis, I.; Yamaguchi, K.; Gordon, A.; Carlson, R.; Brent, R. Using Protein-DNA Chimeras To Detect and Count Small Numbers of Molecules. *Nat. Methods* **2005**, *2*, 31–37.
12. Cecconi, C.; Shank, E. A.; Dahlquist, F. W.; Marqusee, S.; Bustamante, C. Protein-DNA Chimeras for Single Molecule Mechanical Folding Studies with the Optical Tweezers. *Eur. Biophys. J.* **2008**, *37*, 729–738.
13. Rothemund, P. W. Folding DNA To Create Nanoscale Shapes and Patterns. *Nature* **2006**, *440*, 297–302.
14. Kolb, H. C.; Finn, M. G.; Sharpless, K. B. Click Chemistry: Diverse Chemical Function from a Few Good Reactions. *Angew. Chem., Int. Ed.* **2001**, *40*, 2004–2021.
15. van Dongen, S. F.; Teeuwen, R. L.; Nallani, M.; van Berkel, S. S.; Cornelissen, J. J.; Nolte, R. J.; van Hest, J. C. Single-Step Azide Introduction in Proteins *via* an Aqueous Diazo Transfer. *Bioconjugate Chem.* **2009**, *20*, 20–23.
16. Wang, L.; Schultz, P. G. Expanding the Genetic Code. *Angew. Chem., Int. Ed.* **2004**, *44*, 34–66.
17. Wang, L.; Brock, A.; Herberich, B.; Schultz, P. G. Expanding the Genetic Code of *Escherichia coli*. *Science* **2001**, *292*, 498–500.
18. Cellitti, S. E.; Jones, D. H.; Lagpacan, L.; Hao, X. S.; Zhang, Q.; Hu, H. Y.; Brittain, S. M.; Brinker, A.; Caldwell, J.; Bursulaya, B.; *et al. In Vivo* Incorporation of Unnatural Amino Acids To Probe Structure, Dynamics, and Ligand Binding in a Large Protein by Nuclear Magnetic Resonance Spectroscopy. *J. Am. Chem. Soc.* **2008**, *130*, 9268–9281.
19. Lallana, E.; Riguera, R.; Fernandez-Megia, E. Reliable and Efficient Procedures for the Conjugation of Biomolecules through Huisgen Azide-Alkyne Cycloadditions. *Angew. Chem., Int. Ed.* **2011**, *50*, 8794–8804.
20. Los, G. V.; Encell, L. P.; McDougall, M. G.; Hartzell, D. D.; Karassina, N.; Zimprich, C.; Wood, M. G.; Learish, R.; Ohana, R. F.; Urh, M.; *et al.* Halotag: A Novel Protein Labeling Technology for Cell Imaging and Protein Analysis. *ACS Chem. Biol.* **2008**, *3*, 373–382.
21. Popa, I.; Berkovich, R.; Alegre-Ceballada, J.; Badilla, C. L.; Rivas-Pardo, J. A.; Taniguchi, Y.; Kawakami, M.; Fernandez, J. M. Nanomechanics of Halotag Tethers. *J. Am. Chem. Soc.* **2013**, *135*, 12762–12771.
22. Keppler, A.; Kindermann, M.; Gendreizig, S.; Pick, H.; Vogel, H.; Johnsson, K. Labeling of Fusion Proteins of O6-Alkylguanine-DNA Alkyltransferase with Small Molecules *in Vivo* and *in Vitro*. *Methods* **2004**, *32*, 437–444.
23. Yin, J.; Straight, P. D.; McLoughlin, S. M.; Zhou, Z.; Lin, A. J.; Golan, D. E.; Kelleher, N. L.; Kolter, R.; Walsh, C. T. Genetically Encoded Short Peptide Tag for Versatile Protein Labeling by Sfp Phosphopantetheinyl Transferase. *Proc. Natl. Acad. Sci. U.S.A.* **2005**, *102*, 15815–15820.
24. Maillard, R. A.; Chistol, G.; Sen, M.; Righini, M.; Tan, J.; Kaiser, C. M.; Hodges, C.; Martin, A.; Bustamante, C. Clpx(P) Generates Mechanical Force to Unfold and Translocate Its Protein Substrates. *Cell* **2011**, *145*, 459–469.
25. Yin, J.; Lin, A. J.; Golan, D. E.; Walsh, C. T. Site-Specific Protein Labeling by Sfp Phosphopantetheinyl Transferase. *Nat. Protoc.* **2006**, *1*, 280–285.
26. Wong, L. S.; Thirlway, J.; Micklefield, J. Direct Site-Selective Covalent Protein Immobilization Catalyzed by a Phospho-pantetheinyl Transferase. *J. Am. Chem. Soc.* **2008**, *130*, 12456–12464.
27. Wong, L. S.; Karthikeyan, C. V.; Eichelsdoerfer, D. J.; Micklefield, J.; Mirkin, C. A. A Methodology for Preparing Nano-structured Biomolecular Interfaces with High Enzymatic Activity. *Nanoscale* **2012**, *4*, 659–666.
28. Limmer, K.; Pippig, D. A.; Aschenbrenner, D.; Gaub, H. E. A Force-Based, Parallel Assay for the Quantification of Pro-tein-DNA Interactions. *PLoS One* **2014**, *9*, No. e89626.
29. Kufer, S. K.; Strackharn, M.; Stahl, S. W.; Gumpp, H.; Puchner, E. M.; Gaub, H. E. Optically Monitoring the Mechanical Assembly of Single Molecules. *Nat. Nanotechnol.* **2009**, *4*, 45–49.
30. Kinkhabwala, A. A.; Yu, Z. F.; Fan, S. H.; Moerner, W. E. Fluorescence Correlation Spectroscopy at High Concen-trations Using Gold Bowtie Nanoantennas. *Chem. Phys.* **2012**, *406*, 3–8.
31. Heucke, S. F.; Baumann, F.; Acuna, G. P.; Severin, P. M.; Stahl, S. W.; Strackharn, M.; Stein, I. H.; Altpeter, P.; Tinnefeld, P.; Gaub, H. E. Placing Individual Molecules in the Center of Nanoapertures. *Nano Lett.* **2014**, *14*, 391–395.
32. Heucke, S. F.; Puchner, E. M.; Stahl, S. W.; Holleitner, A. W.; Gaub, H. E.; Tinnefeld, P. Nanoapertures for AFM-Based Single-Molecule Force Spectroscopy. *Int. J. Nanotechnol.* **2013**, *10*, 607–619.

Supporting Information

Protein-DNA Chimeras for Nano Assembly

Diana A. Pippig[1],*, Fabian Baumann[1], Mathias Strackharn[1], Daniela Aschenbrenner[1,2],

Hermann E. Gaub[1]

[1]Center for Nanoscience and Department of Physics, University of Munich,

Amalienstraße 54, 80799 Munich, Germany

[2]Center for Integrated Protein Science Munich

*diana.pippig@physik.lmu.de

The experiments described in the manuscript were performed on an AFM/TIRFM hybrid, the details of which may be found in Gumpp et al.[1] This supporting information specifies methods and materials that are relevant for the conduction of the measurements discussed in the main text.

AFM Measurements

A custom built AFM head and an Asylum Research MFP3D controller (Asylum Research, Santa Barbara, USA), which provides ACD and DAC channels as well as a DSP board for setting up feedback loops, were used. Software for the automated control of the AFM head and xy-piezos during the SMC&P experiments was programmed in Igor Pro (Wave Metrics, Lake Oswego, USA). MLCT-AUHW cantilevers (Bruker, Camarillo, USA; 20 nm nominal tip radius, pyramidal shaped probe) and BioLever Mini (BL-AC40TS, here "BLM") cantilevers (Olympus, Japan; 10 nm nominal tip radius, sharpened probe) were chemically modified (see Preparation of Cantilevers) and calibrated in solution using the equipartition theorem.[2,3] Pulling velocities were set to 2 µm/s in the depot and 0.2 µm/s in the target area. The positioning feedback accuracy is ±3 nm. However, long-term deviations may arise due to thermal drift. Typical times for one Cut & Paste cycle amount to approximately 3 s in these experiments.

TIRF Microscopy

The fluorescence microscope of the hybrid instrument excites the sample through the objective in total internal reflection mode. A 100x/1.49 oil immersion objective (CFI Apochromat TIRF, Nikon, Japan) was employed. Blue excitation for monitoring GFP fluorescence was achieved with a fiber-coupled 473 nm diode laser (iBEAM smart, Toptica Photonics, Gräfelfing, Germany) at an estimated excitation intensity of approximately 10 W/cm^2. The corresponding filter set consists of z 470/10 (Chroma, Bellows Falls, VT, USA), ND10A (for grid experiments, Thorlabs GmbH, Dachau, Germany), z 470 RDC, HQ 525/50, HQ485lp (all of Chroma, Bellows Falls, VT, USA)

and HC 750/SP (AHF, Tübingen, Germany) filters. Images were recorded with a back-illuminated EMCCD camera (DU-860D, Andor, Belfast, Ireland) in frame transfer mode with 1 MHz readout rate at a frame rate of 10 Hz. The camera was water cooled and operated at -75 °C.

Preparation of the C11L34 Single Chain Antibody Fragment

The C11L34 single chain antibody fragment was prepared as described previously.[4] The scFv construct harbored a C-terminal Hexa-His-tag followed by a Cys to allow for site-specific immobilization and was obtained by periplasmic expression in *E. coli* SB536. C11L34 was purified by Ni^{2+} and immobilized antigen affinity chromatography according to standard protocols. The concentration was adjusted to ~1.4 mg/ml in a storage buffer containing 50 mM sodium phosphate, pH 7.2, 50 mM NaCl and 10 mM EDTA.

Preparation of the ybbR-GFP-GCN4 Construct

A superfolderGFP[5] construct was designed to harbor an N-terminal ybbR-tag (DSLEFIASKLA)[6, 7] and a C-terminal GCN4-tag (YHLENEVARLKKL).[8] The sfGFP gene was PCR amplified from a synthetic template (Lifetechnologies, Paisley, UK) with primers containing the respective tag coding sequences. The construct was cloned into a modified pGEX6P2 vector (GE Healthcare, Little Chalfont, UK) that, in addition to the GST-tag, harbors a Hexa-His-Tag and a TEV-Protease cleavage site, by means of NdeI and XhoI restriction sites.

The resulting fusion protein (ybbR-sfGFP-GCN4) harbored a GST- as well as a Hexa-His-tag and was expressed in *E.coli* BL21 DE3 CodonPlus cells (Agilent Technologies, Inc., Santa Clara, CA, USA). For this, one liter of SB medium was inoculated with 10 ml of an overnight culture and grown at 37°C. When an OD_{600} of 0.7 had been reached, over night expression at 18°C was induced by adding 0.25mM IPTG.

Cells were lysed in 50mM Tris HCl pH 7.5, 150 mM NaCl, 2mM DTT, 5% Glycerol, by a French pressure cell press. The ybbR-sfGFP-GCN4 construct was obtained in the soluble fraction and purified by Glutathione affinity chromatography on a GSTrap column (GE Healthcare, Little Chalfont, UK). After over night incubation with PreScission protease the GST-tag was removed and the protein further purified by Ni-IMAC over a HisTrap HP column (GE Healthcare, Little Chalfont, UK). The purified protein was concentrated and the buffer exchanged (50mM Tris HCl pH7.5, 150mM NaCl, 2mM DTT, 5% Glycerol) by ultrafiltration in 10 kDa MWCO Amicon centrifuge filter devices (EMD Millipore Corporation, Billerica, MA, USA). Protein was stored at -80°C at a final concentration of 6.5 µM.

Sfp-mediated Coupling of Coenzyme A-modified DNA to ybbR-GFP-GCN4

3'-Coenzyme A-modified transfer DNA was synthesized by biomers.net GmbH (Ulm, Germany). Lyophilized DNA was dissolved in Sfp-buffer (120 mM TrisHCl pH7.5, 10 mM $MgCl_2$, 150 mM NaCl, 2% Glycerol, 2 mM DTT) to a concentration of 100 mM. The coupling reaction was slightly altered from Yin *et al.*[6] by mixing 10 nmol CoA-DNA with 7.2 nmol ybbR-GFP-GCN4 and 0.75 nmol Sfp in a total volume of 1.5 ml in Sfp-buffer. The mix was incubated at room temperature and the progress of the reaction was

followed by analyzing aliquots in SDS-PAGE. Best coupling efficiency (ca. 90%) was achieved after concentrating the entire reaction mix 10fold by ultrafiltration and over night incubation at room temperature. To remove remaining free DNA, the GFP-DNA construct was further purified by anion exchange chromatography (Suppl. Fig. S1a) on a HiTrap Q HP column (GE Healthcare, Little Chalfont, UK). Fractions were analyzed by SDS-PAGE (Suppl. Fig. S1b) and UV/Vis spectrometry at 260, 280 and 488 nm. Aliquots of 3.8 μM DNA/GFP-GCN4 conjugate were stored at -80°C.
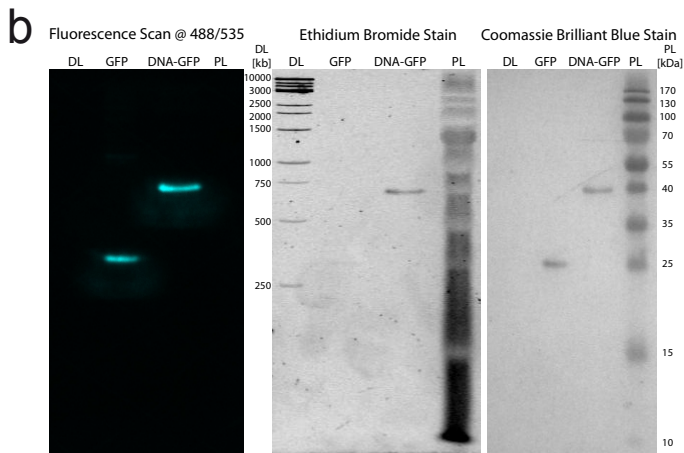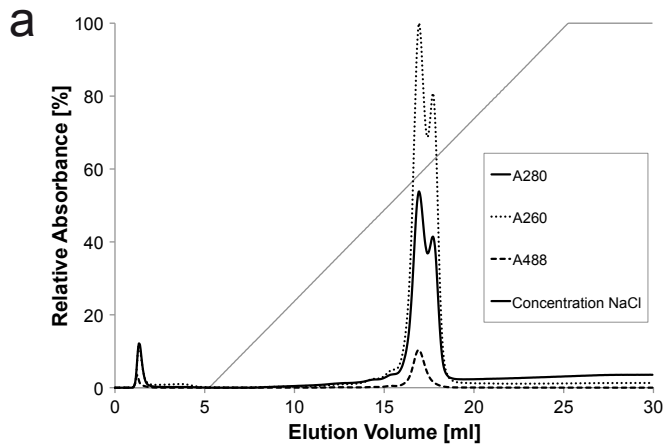
Supplementary Figure S1. Purification of the covalent GFP-DNA complex. (a) Chromatogram of the anion exchange chromatography and (b) SDS-PAGE gel imaged by fluorescence scan (excitation 488 nm, emission 535 nm), after Ethidium Bromide staining and UV detection and after Coomassie Staining. Samples loaded were: "DL" – DNA-ladder 1kb ruler (ThermoFisher Scientific, Waltham, MA, USA), "GFP" – ybbR-sfGFP-GCN4 , "DNA-GFP" – DNA-CoA-ybbR-sfGFP-GCN4, "PL" – Protein ladder PAGERuler Prestained (ThermoFisher Scientific, Waltham, MA, USA).

Preparation of Cantilevers

Cantilevers (MLCT obtained from Asylum Research, Santa Barbara, CA and BioLever Mini obtained from Olympus, Japan) were oxidized in a UV-ozone cleaner (UVOH 150 LAB, FHR Anlagenbau GmbH, Ottendorf-Okrilla, Germany) and silanized by soaking for 2 min in (3-Aminopropyl)dimethylethoxysilane (ABCR, Karlsruhe, Germany; 50% v/v in Ethanol) . Subsequently, they were washed in toluene, 2-propanol and ddH$_2$O and dried at 80 °C for 30 min. After incubating the cantilevers in sodium borate buffer (pH 8.5), a heterobifunctional PEG crosslinker[9] with N-hydroxy succinimide and maleimide groups (MW 5000, Rapp Polymere, Tübingen, Germany) was applied for 1 h at 25 mM in sodium borate buffer. Afterwards, the C11L34 antibody fragments were bound to the cantilevers at 8 °C for 2-4 h. Finally the cantilevers were washed and stored in PBS.

Preparation of Glass Surfaces

Glass cover slips were sonicated in 50% (v/v) 2-propanol in ddH$_2$0 for 15 min and oxidized in a solution of 50% (v/v) hydrogen peroxide (30%) and sulfuric acid for 30 min. They were then washed in ddH$_2$O, dried in a nitrogen stream and then silanized by soaking for 1 h in (3-Aminopropyl)dimethylethoxysilane (ABCR, Karlsruhe, Germany, 1.8 % v/v in Ethanol). Subsequently, they were washed twice in 2-propanol and ddH$_2$O and dried at 80 °C for 40 min. After incubation in sodium borate buffer (pH 8.5), a heterobifunctional PEG crosslinker with N-hydroxy succinimide and maleimide groups (MW 5000, Rapp Polymere, Tübingen, Germany) was applied for 1 h at 50 mM in sodium borate buffer. Depot and Target DNA was reduced with TCEP and then purified by ethanol precipitation. DNA pellets were dissolved in phosphate buffer (pH 7.2, 50 mM

NaCl, 10 mM EDTA). A microfluidic system was fixed on the PEGylated cover glass, and the depot and target DNA oligonucleotides were pumped through the two respective channels and incubated for 1 h. Subsequently both channels were flushed with 1mg/ml BSA and then PBS. The GFP-DNA chimera was pumped into the depot channel and incubated for 60 min. The channel was then rinsed again with PBS and the microfluidic system was removed.

SMC&P Experiment

Grid patterns were written in 64 cycles with 1.5 μm space between each deposition point. The denser snowflake pattern was written in 552 transfer cycles. The pulling speed in the depot was set to 2 μm/s and in the target to 0.2 μm/s. This corresponds to approximate surface contact times[10] (dependent on approach/retraction velocity, indentation force and substrate stiffness) of 8 ms and 80 ms, respectively, and should allow for ligand binding (compare $k_{on}(DNA) > 10^4 \, M^{-1} s^{-1}$ and $k_{on}(AB) \sim 10^6 \, M^{-1} s^{-1}$).[10-13] Considering a single antibody molecule being bound to the cantilever tip and estimating its localization in a half sphere with r= 30 nm (length of PEG linker), the local concentration of antibody would be in the mM range. This is several orders of magnitude higher than the K_d for the antibody-peptide interaction (pM to nM range - Berger *et al.*; FEBS, 1999). Taking further into account that bond formation is not diffusion-limited for the SMC&P experiment, successful attachment is very likely even at the given, short contact times. In addition, it is crucial for the respective interactions to be thermally stable over a long time span. Especially the DNA storage bonds in the depot site as well as in the construction

site are required to not passively dissociate. Judging from the extremely low expected off-rates (k_{off}(DNA)>10^{-10} s^{-1}, k_{off}(AB)~10^{-4} s^{-1})[4, 14] this prerequisite should be fulfilled. One SMC&P cycle is completed in less than 3 s, this is mainly dependent on the pulling speed, which is optimized with respect to loading rates and thus rupture forces. This warrants that the zipper-DNA storage bond is more likely to rupture during the pickup process than the newly formed antibody – GCN4-peptide bond, whereas the shear-DNA bond formed in the deposition process is more likely to withstand the final retraction. The functionalization density of the cantilever, depot and target region was adjusted to allow for high effectiveness in SMC&P. Transfer efficiencies were determined from rupture events and forces (Fig. 2, 3, Suppl. Fig. S3) as well as fluorescence intensity traces (Fig. 2) of transported GFP molecules over time.

Rupture forces and loading rates were evaluated from AFM force distance curves that were recorded for each pick-up and deposition process (moving average smoothing over 5 data points was employed for improved visualization in Fig. 2, but not evaluation) utilizing a quantum mechanically corrected WLC model[15] (force spectroscopy data was evaluated in Igor Pro).

Fluorescence bleaching of deposited molecules in a 2x2 pixel area (180 nm/pixel), corresponding to the 4 brightest pixels in the expected deposition vicinity, was followed for 200 s at 0.1 s exposure time. Smoothing, by moving average over five data points, for improved bleaching step perceptibility and analysis were performed in ImageJ. Where applicable, *i.e.* with the number of transported GFP molecules being in an, in our hands, resolvable range in the time course experiments (for BLM grids), exact numbers of

deposited GFP molecules could be deduced from bleaching steps in the fluorescence traces (Fig. 2, Suppl. Fig. S2 – traces not shown).

For MLCT cantilevers the transfer efficiency ranged around 20 (as found for the snowflake pattern; deduced from rupture forces Fig. 3) molecules per cycle. For the sharp-tipped BLM cantilevers functionalization conditions were limiting, so that mainly single molecules were transported and not all SMC&P cycles resulted in a deposition (Fig. 2, Suppl. Fig. S2)
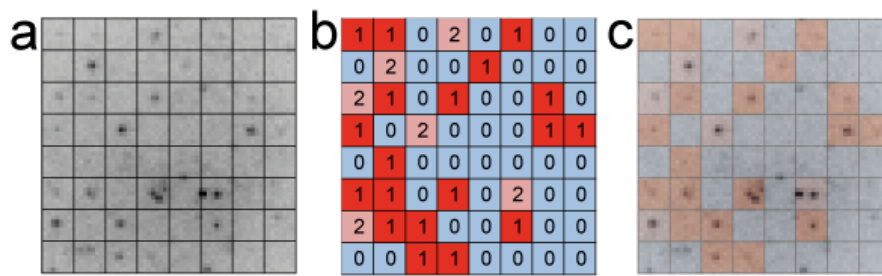
Supplementary Figure S2. Representative 8x8 deposition point grid pattern of a GFP SMC&P experiment employing a BLM cantilever. (a) The TIRFM image represents the standard deviation of the fluorescence within the recorded series as evaluated with ImageJ (exemplary BLM 8x8 grid: first 774 frames at 0.1 s exposure time). (b) The number of deposited GFP molecules in each grid position was determined from fluorescence signals over time in 2x2 pixel areas, representative of the 4 brightest pixels in the approximated deposition vicinity. (c) Superposition of the TIRFM image and the color-coded deposition count panel (blue - 0, red – 1, pale red - 2 GFP molecules).
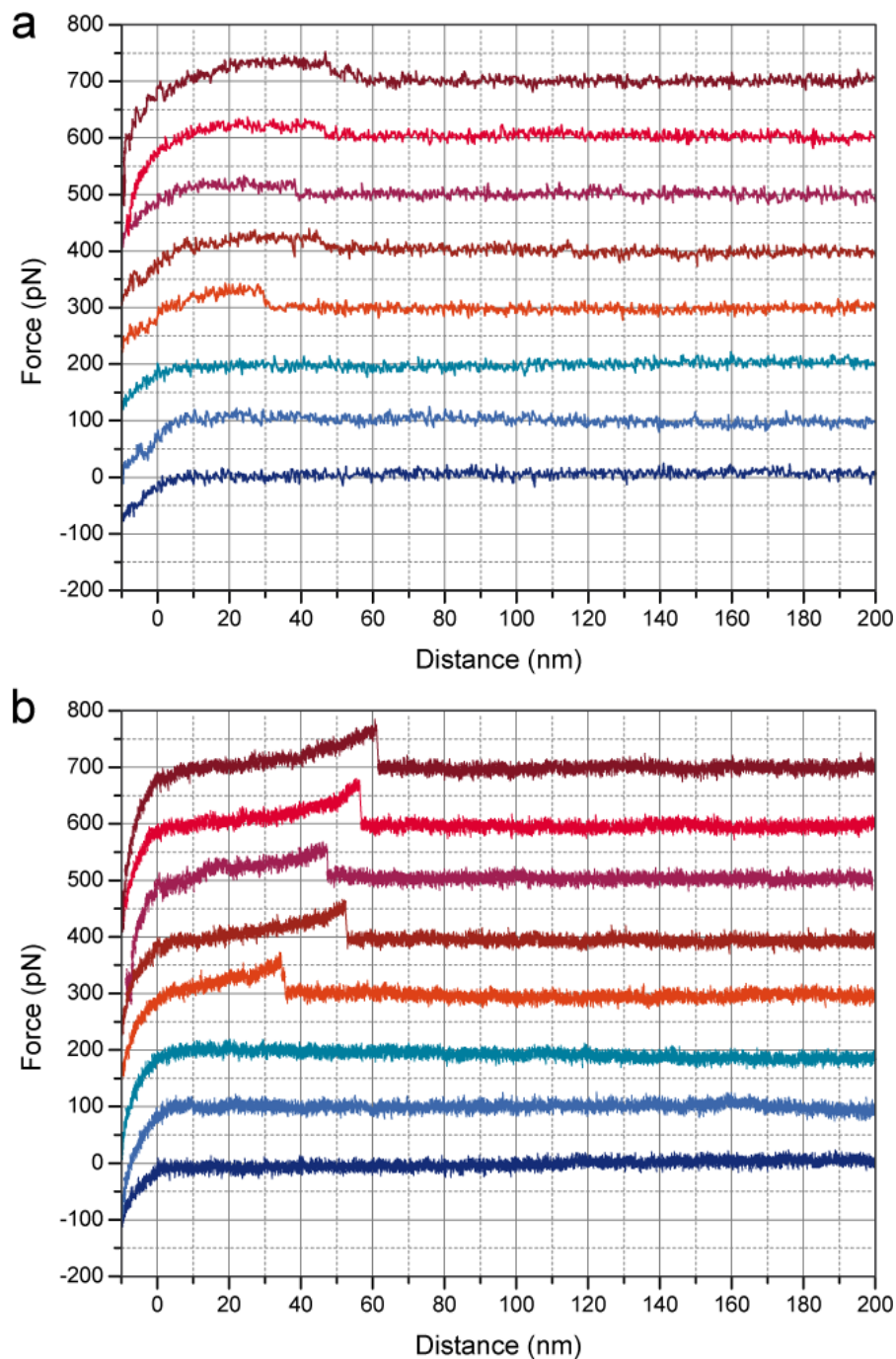
Supplementary Figure S3. Representative example curves of GFP SMC&P experiments

employing BLM cantilevers. Curves that represent no rupture, *i.e.* no pick-up or deposition events

are depicted in tints of blue. Single-event curves are shown in tints of red. (a) Single-event depot

rupture forces range around 20 pN (corresponding with the unzipping of the DNA storage

bond)[16], (b) whereas single-event target rupture forces range around 50 pN, which resembles the

rupture of a single anti-GNC4 antibody/GCN4-peptide interaction at the observed loading rates of

~300 pN/s.[4]

Oligomer Sequences

thiolated depot oligomer

5' SH - TTT TTT CAT GCA AGT AGC TAT TCG AAC TAT AGC TTA AGG ACG TCA A

thiolated target oligomer

5' CAT GCA AGT AGC TAT TCG AAC TAT AGC TTA AGG ACG TCA ATT TTT T– SH

CoA-modified transfer oligomer for protein coupling

5' TTG ACG TCC TTA AGC TAT AGT TCG AAT AGC TAC TT G CAT GTT TTT TTT TTT TTT-

CoA 3'

References

1.   Gumpp, H.; Stahl, S. W.; Strackharn, M.; Puchner, E. M.; Gaub, H. E. Ultrastable Combined Atomic Force and Total Internal Reflection Fluorescence Microscope [Corrected]. *Rev. Sci. Instrum.* 2009, 80, 063704.
2.   Florin, E. Sensing Specific Molecular Interactions with the Atomic Force Microscope. *Biosens. Bioelectron.* 1995, 10, 895-901.
3.   Butt, H. J.; Jaschke, M. Calculation of Thermal Noise in Atomic-Force Microscopy. *Nanotechnology* 1995, 6, 1-7.
4.   Morfill, J.; Blank, K.; Zahnd, C.; Luginbuhl, B.; Kuhner, F.; Gottschalk, K. E.; Pluckthun, A.; Gaub, H. E. Affinity-Matured Recombinant Antibody Fragments Analyzed by Single-Molecule Force Spectroscopy. *Biophys. J.* 2007, 93, 3583-3590.
5.   Pedelacq, J. D.; Cabantous, S.; Tran, T.; Terwilliger, T. C.; Waldo, G. S. Engineering and Characterization of a Superfolder Green Fluorescent Protein. *Nat. Biotechnol.* 2006, 24, 79-88.
6.   Yin, J.; Lin, A. J.; Golan, D. E.; Walsh, C. T. Site-Specific Protein Labeling by Sfp Phosphopantetheinyl Transferase. *Nat. Protoc.* 2006, 1, 280-285.
7.   Yin, J.; Straight, P. D.; McLoughlin, S. M.; Zhou, Z.; Lin, A. J.; Golan, D. E.; Kelleher, N. L.; Kolter, R.; Walsh, C. T. Genetically Encoded Short Peptide Tag for Versatile Protein Labeling by Sfp Phosphopantetheinyl Transferase. *Proc. Natl. Acad. Sci. USA* 2005, 102, 15815-15820.
8.   Strackharn, M.; Stahl, S. W.; Severin, P. M.; Nicolaus, T.; Gaub, H. E. Peptide-Antibody Complex as Handle for Single-Molecule Cut & Paste. *ChemPhysChem* 2012, 13, 914-917.
9.   Celik, E.; Moy, V. T. Nonspecific Interactions in Afm Force Spectroscopy Measurements. *J. Mol. Recognit.* 2012, 25, 53-56.
10.   Guo, S.; Lad, N.; Ray, C.; Akhremitchev, B. B. Association Kinetics from Single Molecule Force Spectroscopy Measurements. *Biophys. J.* 2009, 96, 3412-3422.
11.   Tawa, K.; Yao, D.; Knoll, W. Matching Base-Pair Number Dependence of the Kinetics of DNA-DNA Hybridization Studied by Surface Plasmon Fluorescence Spectroscopy. *Biosens. Bioelectron.* 2005, 21, 322-329.
12.   Henry, M. R.; Wilkins Stevens, P.; Sun, J.; Kelso, D. M. Real-Time Measurements of DNA Hybridization on Microparticles with Fluorescence Resonance Energy Transfer. *Anal. Biochem.* 1999, 276, 204-214.
13.   Berger, C.; Weber-Bornhauser, S.; Eggenberger, J.; Hanes, J.; Pluckthun, A.; Bosshard, H. R. Antigen Recognition by Conformational Selection. *FEBS Lett.* 1999, 450, 149-153.
14.   Strunz, T.; Oroszlan, K.; Schafer, R.; Guntherodt, H. J. Dynamic Force Spectroscopy of Single DNA Molecules. *Proc. Natl. Acad. Sci. USA* 1999, 96, 11277-11282.
15.   Hugel, T.; Rief, M.; Seitz, M.; Gaub, H. E.; Netz, R. R. Highly Stretched Single Polymers: Atomic-Force-Microscope Experiments *Versus* Ab-Initio Theory. *Phys. Rev. Lett.* 2005, 94, 048301.
16.   Rief, M.; Clausen-Schaumann, H.; Gaub, H. E. Sequence-Dependent Mechanics of Single DNA Molecules. *Nat. Struct. Biol.* 1999, 6, 346-349.